Spatial and depth distribution of salinity and nitrate in a depleted alluvial aquifer (Haouz plain, Morocco)

Hamza Sahraoui, Younes Fakir, Houssne Bouimouass, Sarah Tweed, Marc Leblanc, Rabia Benaddi, Abdelghani Chehbouni

Journal of Hydrology: Regional Studies 57 (2025) 102143

Contents lists available at ScienceDirect

Journal of Hydrology: Regional Studies

journal homepage: www.elsevier.com/locate/ejrh

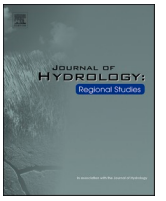

Spatial and depth distribution of salinity and nitrate in a depleted alluvial aquifer (Haouz plain, Morocco)

Hamza Sahraoui [a], Younes Fakir [a,b,*,1], Houssne Bouimouass [b], Sarah Tweed [c], Marc Leblanc [d], Rabia Benaddi [e], Abdelghani Chehbouni [b,f]

[a] Geosciences Semlalia laboratory, Cadi Ayyad University, Marrakech, Morocco
[b] CRSA, Center for Remote Sensing Applications, Mohammed VI Polytechnic University, Ben Guerir, Green City, Morocco
[c] UMR G-eau, IRD, Montpellier, France
[d] University of Avignon, France
[e] ABHT, Agence du Bassin Hydraulique du Tensift, Marrakech, Morocco
[f] CESBIO, UMR IRD, Toulouse, France

ARTICLE INFO

Keywords:
Groundwater depletion
Geochemical processes
Nitrate levels
Arid
Tensift basin

ABSTRACT

Understanding groundwater contamination processes in depleted aquifers is needed to improve their integrated management. The present study aims to understand how the conditions prevailing in a depleting detritic unconfined aquifer could affect the salinity and nitrate contamination. The depletion has caused a shift in our alluvial aquifer from dominant very shallow groundwater (< 20 m) in the 1970s to dominant deep groundwater (> 40 m) currently. It was found that (i) groundwater was moderately affected by salinity and nitrate, (ii) the dominant hydrochemical factors are rock weathering, halite dissolution, and reverse ion exchange, and (iii) the nitrate contamination is higher in shallow groundwater but it was detected at all depths. The thick unsaturated zone, which has developed because of the decline of the water table, would have mitigated the surface-borne contamination and reduced the direct effects of evapotranspiration. Using tritium as age indicator, it was suggested that nitrate in deep groundwater could originate from a historical use of fertilizers. In addition, vertical flows induced by decreasing water-table from pumping could transport younger groundwater with high loads of nitrate to mix with older deep groundwater with low nitrate. Serious problems could arise from further mobilization of salts by pumping deep groundwater and from the effects of downward movement of contaminants accumulated in the thick unsaturated zone after sufficient migration time or increases in groundwater recharge rates.

1. Introduction

Groundwater is the main source of water supply in many countries, especially in arid and semiarid regions (Margat and Van der Gun, 2013). In recent decades, groundwater withdrawals have increased excessively to meet human water demand for drinking water, especially in rural areas (Yu et al., 2020; Subba Rao et al., 2020; Soleimani et al., 2020), and more broadly for irrigation, which consumes more than 40 % of global groundwater resources (Marston et al., 2015; Wada and Bierkens, 2014). In many (semi)arid

* Correspondence to: Geosciences Semlalia laboratory, Cadi Ayyad University, Bd. Prince My Abdellah, PO box 2390, Marrakech 40000, Morocco.
E-mail address: fakir@uca.ac.ma (Y. Fakir).
[1] ORCID ID: https://orcid.org/0000-0003-4299-5862

https://doi.org/10.1016/j.ejrh.2024.102143
Received 22 March 2024; Received in revised form 12 December 2024; Accepted 16 December 2024
Available online 26 December 2024

agricultural regions of the world, this has led to long-term overexploitation of groundwater, resulting in aquifers' depletion (Fishman et al., 2011; Wada et al., 2010; Gerten et al., 2013; Rosa et al., 2018), with various negative impacts on ecohydrological systems and human-related services. Furthermore, in (semi)arid agricultural regions the groundwater quality is seriously threatened by salinization

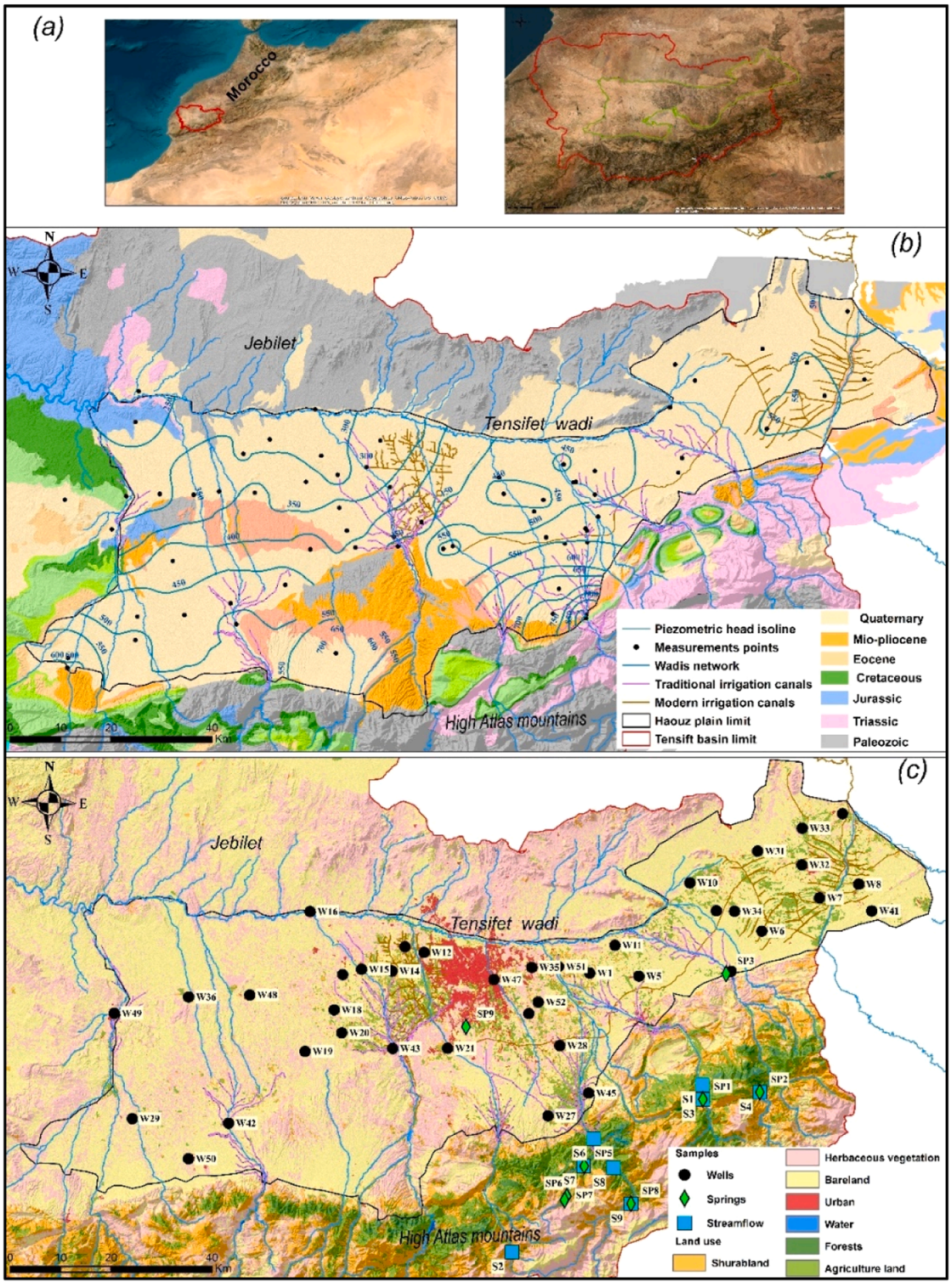

Fig. 1. Location of the study area (a), geological map with piezometric isolines of the alluvial aquifer (b), land use map with the sampled wells in the plain and the sampled spring and streamflow in the mountains (c).

(Abuelgasim and Ammad, 2018; Singh, 2019) and by nitrate contamination (Gu et al., 2013). Groundwater salinity in arid environments could be increased by leaching from salinized soils (Wang et al., 2021), irrigation with saline water (Gowing et al., 2009), and concentration of salts owing to plant water uptake and/or evaporation (Ghalib, 2017; Rajmohan et al., 2021) especially when the water table is very shallow (Shah et al., 2007). Nitrate is the most common chemical contaminant in the world's aquifers due to its solubility in water and difficulty of fixation in soil (Bhatnagar and Sillanpää, 2011; Abascal et al., 2022). Its high concentration in groundwater is a significant concern because of its complex origin and harmful effects on human health (Gan et al., 2022). It is often associated with the use of nitrogenous fertilizers and livestock in agricultural areas (Liu et al., 2024) and sewage systems in populated and urbanized areas (Kapembo et al., 2016; Puig et al., 2017; Huang et al., 2018; Blarasin et al., 2020, Zhang et al., 2020).

Groundwater depletion causes quantitative changes in aquifers, including water-table decline, loss of groundwater reserves, reduction of groundwater discharge to springs, streams, and wetlands, drying up or reduction of well yields, and land subsidence (Konikow, 2015; Kummu et al., 2016; Xanke and Liesch, 2022). Depletion may also induce changes in groundwater quality. The most documented is seawater intrusion into coastal aquifers. The lowering of the water table allows the landward movement of seawater, which contaminates coastal aquifers and increases their salinity (e.g., Benkabbour et al., 2004; Badaruddin et al., 2015; Werner, 2017; Prusty and Farooq, 2020). In addition to seawater intrusion, two other contamination processes can be expected in depleting aquifers. The first one is related to the installation of deep pumping wells to extract deep groundwater. Due to declining water tables, new deep wells are often drilled or existing wells are deepened as shallow wells dry up or provide lower yields (Perrone and Jasechko, 2019). Those new deep wells could pierce adjacent geological formations of higher water salinity and cause saline water contaminate aquifers (Andreu et al., 2008; Rodriguez-Estrella, 2014). The geological formations could lie at the bottom of an aquifer and contain evaporite deposits, typically gypsum or halite (Salameh and Hammouri, 2008; Andreu et al., 2008; Rodriguez-Estrella, 2014), or connate salt in porewater (Ait Lemkademe et al., 2022). The second process could be triggered by heavy pumping of groundwater. Using groundwater quality data and indicators of groundwater age (residence time), studies have suggested that vertical flow becomes dominant within an aquifer under heavy pumping, so that modern shallow groundwater, which is often contaminated, is likely to move deeper and transport contaminants (including nitrate) to old deep groundwater, which is normally less vulnerable to surface contamination (Burow et al., 2007; Lapworth et al., 2017).

Given the global extent of groundwater depletion, in addition to the quantitative assessments, it is vital to address the contamination processes in depleting aquifers in order to contribute to their integrated management. The main objective of the present study is to understand how the conditions prevailing in a depleting detritic unconfined aquifer could affect the salinity and especially nitrate contamination processes of the currently pumped groundwater. Detritic unconfined aquifers, especially those of alluvial sediments, often have good permeability and productivity due to the presence of coarse material (Baillieux et al., 2014). In addition, they are easily accessible and therefore the most exploited type of aquifer (Aureli et al., 2008; Mukherjee et al., 2015), and hence the most exposed to overexploitation to meet irrigation needs in (semi)arid agricultural areas. We performed geochemical investigations and focused on how salinity and nitrate content vary between shallow and deeper groundwater of the alluvial aquifer. Tritium data were used to trace the age of groundwater at different depths in the aquifer and relate it to nitrate contamination processes.

2. Materials and methods

2.1. Study area

The study area spans across the Haouz plain, which covers 6000 km^2 in the Tensift basin of Central Morocco (Fig. 1a). This vast plain encompasses the city of Marrakech (Fig. 1b), home to approximately 1 million people. The regional economy is primarily based on agriculture and tourism. The climate in the plain is arid, with an average annual rainfall of 195 mm and potential evapotranspiration (Hargreaves) of 1616 mm in Marrakech city over the period of 2005–2021.

Since the 2000s, the Haouz plain has experienced a rapid expansion of irrigated agriculture, supported by several national government programs (Ouassanouan et al., 2022). Irrigated crops are primarily olive trees, citrus, wheat, and vegetables, which are irrigated using surface water and groundwater. The surface waters consist of intermittent and ephemeral wadis (streams) originating from the High-Atlas mountains, which receive higher precipitation (approximately 500 mm annually). The wadis' water is diverted through a network of hundreds of canals in the piedmont to provide traditional irrigation (see Fig. 1c). Additionally, two dams supply

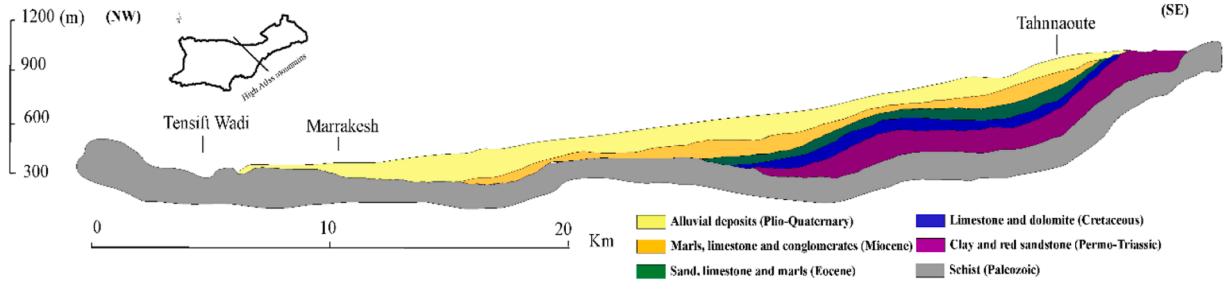

Fig. 2. Synthetic geological cross-section through the Haouz Plain (based on Bernet and Prost, 1975). The bottom of the alluvial aquifer is primarily composed of Miocene marls, along with Triassic clays and Paleozoic schists in the margines of the plain.

some irrigated perimeters via modern concrete canals. Groundwater is often the primary source of irrigation water, especially during droughts. It is also the sole source of irrigation for large areas that are not covered by surface water networks.

The study has targeted the unconfined aquifer beneath the Haouz plain, which consists mainly of Neogene and Quaternary detrital alluvial deposits (Fig. 1b), largely derived from the erosion of the High-Atlas mountains during their gradual uplift. These deposits are formed of silt, conglomerate, sandstone, marl and lacustrine limestone (in Bernet and Prost, 1975), and their thickness can reach more than 150 m (Kamal et al., 2021). The Miocene marls form the aquitard (Fig. 2) that separates the alluvial unconfined aquifer from Eocene and Cretaceous carbonate deep layers. Triassic (sandstone beds and salt deposits) and crystalline Paleozoic terrains border the alluvial deposits laterally and could locally form the aquifer bottom in the East where Triassic deposits are extended and, in the North where the crystalline Paleozoic massif of the Jebilet limits the alluvial aquifer (Fig. 1b, Fig. 2).

The groundwater in the alluvial aquifer was described to flow from the south (High-Atlas mountains) to the north (Tensift stream), and as mainly influenced by wadis that recharge or drain the aquifer (Boukhari et al., 2015). The piezometric isolines drawn in this study (Fig. 1b) exhibited distortions and depressions attributable to the influence of pumping activities on the water-table. Groundwater recharge of the alluvial aquifer occurs mainly in the central piedmont of the High-Atlas mountains. The sources of recharge include streamflow losses (Fakir et al., 2021; Hajhouji et al., 2022), irrigation water via a network of traditional irrigation canals in the piedmont (Bouimouass et al., 2020), and subsurface inflow (Bouimouass et al., 2024).

Recent studies in the plain have shown a significant increase in irrigated crops (Ouassanouan, 2022). Due to a decrease in surface water supplies for both irrigation and groundwater recharge, this has led to a significant intensification of groundwater pumping and,

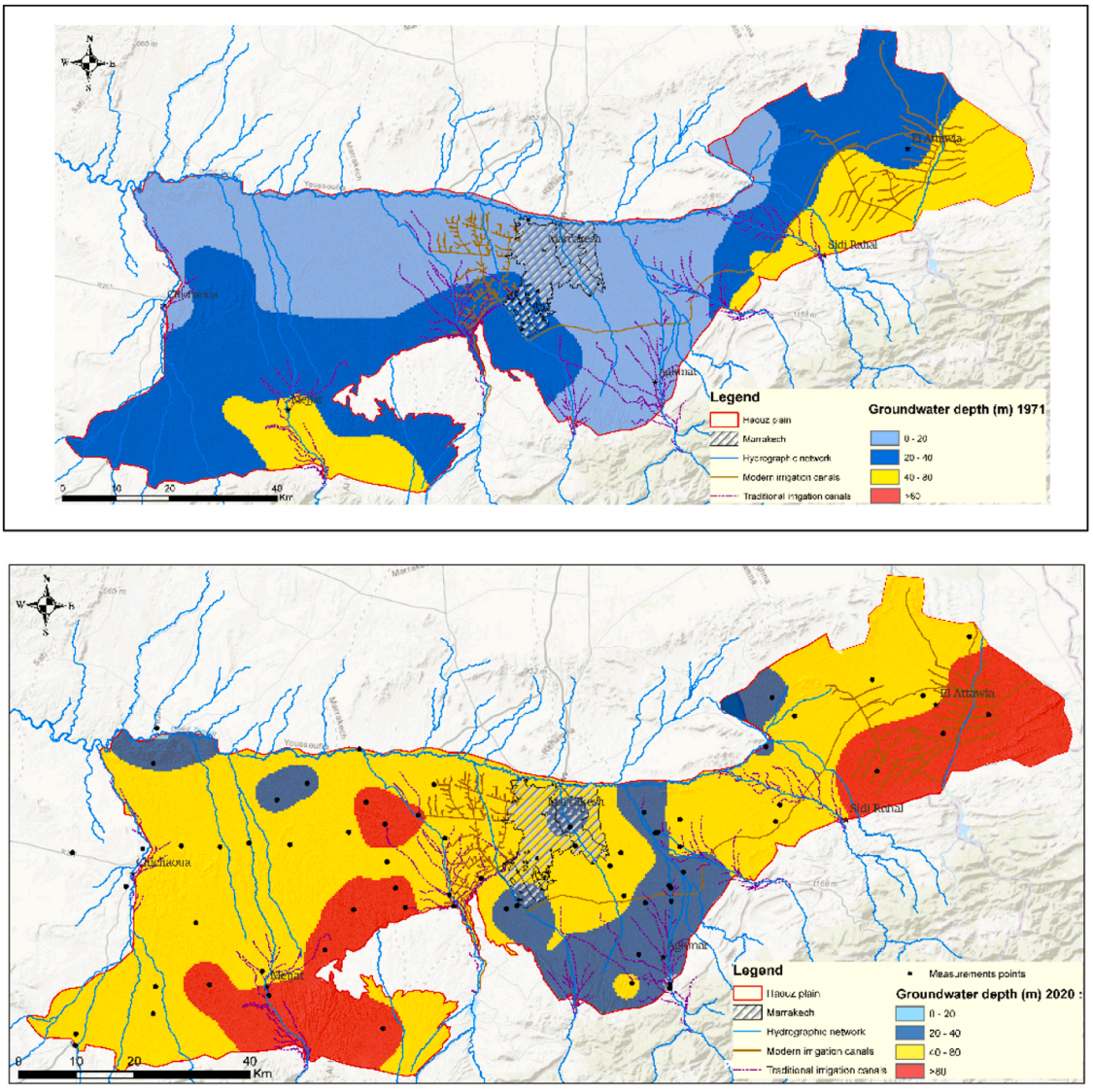

Fig. 3. Depth to water table of the alluvial aquifer in 1971 (top) and in 2020 (down).

consequently, severe groundwater depletion with current water table decline of several meters per year. Fig. 3 shows the dramatic decline of the depth to the water table between 1971 and 2020. In 1971, the very shallow groundwater (depth < 20 m) and the relatively shallow groundwater (20–40 m depth) covered nearly 87 % of the aquifer area, while deep groundwater (40–80 m) was very localized (13 % of the area) and very deep groundwater (> 80 m) was nonexistent. In 2020, the very shallow groundwater has almost disappeared. The shallow groundwater is only found in the central piedmont due to mountain front and irrigation recharge, as well as near some wadis and downstream of the aquifer. The deep groundwater covers a large portion of the plain, occupying 65 % of the area. Very deep groundwater is located in upstream zones at East and West, as well as in the irrigated area of N'Fis, which is one of the most overexploited.

2.2. Sampling, analytical procedures and data

A field campaign was carried out in September-October 2020 to collect water samples for chemical analysis. A total of 63 samples were collected, including surface water (n = 08) and springs (n = 09) from the High-Atlas mountains, and wells (n = 46) tapping the alluvial aquifer of the Haouz plain (Fig. 1c). The objective of the mountain sampling is to show the contrast in salinity and nitrate with the groundwater in the plain. In the latter, the sampling targeted both irrigation and public drinking water wells mostly equipped with pumps. Electrical conductivity (EC) and pH were measured in the field with a portable meter (Hanna instruments). All samples were collected in pre-cleaned polypropylene bottles after at least 30 min of pumping. Samples for cation analyses were filtered in the field (0.45 μm cellulose nitrate filter) and were acidified to pH 2 (ultrapure 16 N HNO3). The samples were analyzed for major cations (Ca^{2+}, Na^{+}, Mg^{2+}, K^{+}), anions (HCO_3^-, Cl^-, SO_4^{2-}), and NO_3^- (Table 1), using ion chromatography (Dionex; ICS1100 and autosampler AS-AP). Tritium analyses were performed for thirty samples a different depth.

2.3. Nitrates limits

To analyze nitrate (NO_3^-) levels in groundwater, three limits or thresholds were considered. According to the World Health Organization drinking water guideline (WHO, 2004), groundwater with concentration of 50 mg/l or higher was considered to be very contaminated and harmful. The value of 25 mg/l NO_3^- (half of the WHO drinking water guideline) is considered here as the lower limit that indicates increasing trends towards harmful contamination. The lower limit of anthropogenic nitrate is based on the assertion that the chemical composition of groundwater can contain one or more populations that may be from geogenic or anthropogenic sources (Manu et al., 2022). These populations are identified here following the method applied in Rahman et al. (2021). The method is based on using the cumulative probability distribution (CPD) of the nitrate dataset to distinguish between the population that may correspond to the natural background concentrations and the one that may correspond to the anthropogenic concentrations of nitrate. This is achieved by identifying a sharp inflection point on the CPD curve separating the two populations. The natural background level of nitrate and the anthropogenic level of nitrate were respectively calculated as the 90th percentile and 10th percentile of the 2 populations. For this analysis, we used a dataset of 78 NO_3^- values measured in the study area: 43 in 2020 in the framework of the present study, and 45 in 2011 (Boukhari et al., 2015).

3. Results and discussion

3.1. Variation of groundwater salinity and geochemical processes

The electrical conductivity (EC) of mountains waters (springs and streamflow) varies from 97 to 2120 μS/cm. The EC of groundwater over the plain is higher, it varies between 438 and 4000 μS/cm, with an average of 1510 μS/cm. According to the classification of Rhoades et al. (1992), the groundwater varies in general from fresh (EC < 700 μS/cm) to slightly saline (700 μS/cm < EC < 2000 μS/cm) (Fig. 4).

The EC of groundwater sampled in the plain decreases slightly with depth (Fig. 5), showing no notable variation between shallow and deep groundwater, apart from the highest groundwater salinity observed in two shallow wells (W2 and W16) and one deep well (W11).

Boxplot diagrams of hydrochemical features (Fig. 6) show that groundwater in the plain is more enriched in major ions than mountains waters. Shallower groundwater (0–40 m) is slightly enriched in major ions than deeper ones and presents a broader range of K^{+}, SO_4^{2-} and NO_3^- concentrations, which can be linked to the impact of anthropogenic activities, especially fertilizers.

As depicted in Fig. 7a and b, groundwater samples predominantly fall within the rock weathering domain of the Gibbs diagram, with slight evaporation effects. Analysis of major ion ratios indicates that the dominant process corresponds to silicate and carbonate dissolution (Fig. 7c and d). Additionally, some groundwater samples are also influenced by evaporite dissolution (Fig. 7d). The most saline shallow groundwater samples are the W2 (EC= 3500 μS/cm) and W16 (EC= 4000 μS/cm). W2 is located near to the Triassic terrains at the limit of the High-Atlas, in the Zat basin known to have important halite deposits. The W16 is located near Tensift Wadi to the East, indicating a probable recharge from this wadi. Water in the Tensift wadi downstream of the city of Marrakech is subject to many sources of high salinity such as the water evacuated from the Paleozoic schists of Draa Sfar mine (Ait Lemkademe et al., 2022) or treated wastewater from the treatment station of Marrakech. The most saline deep groundwater (W11, EC= 2910 μS/cm, depth = 64 m) is located in the East and could also be linked to halite of Triassic deposits of the bottom of the aquifer. Fig. 7e shows that almost all High-Atlas surface waters and some groundwater samples have Na^{+}/Cl^{-} ratios > 1, thus indicating the contribution of silicate weathering. More groundwater samples plot close to Na^{+}/Cl^{-} = 0.8–1, indicating halite dissolution. The most affected samples exhibit

Table 1
Physicochemical parameters of water samples collected in September-October 2020. The concentrations are in mg/l.

Number	Water type	Depth (m)	pH	CE25°C (µS/cm)	HCO_3^-	Cl^-	NO_3^-	SO_4^{2-}	Na^+	K^+	Mg^{2+}	Ca^{2+}	TDS
W1	Groundwater	31,2	8,66	438	195,20	22,45	4,90	10,44	23,47	0,68	11,39	41,21	369
W2	Groundwater	17	8,61	3500	483,12	797,88	64,64	180,32	380,88	10,49	123,92	171,13	3500
W3	Groundwater	93	7,96	1745	551,44	250,91	6,50	65,80	167,67	2,81	51,61	105,29	1745
W5	Groundwater	109	8,66	1605	274,50	386,86	12,28	39,91	169,25	3,12	43,71	73,39	1042
W6	Groundwater	126	8,21	1390	223,26	318,08	15,95	59,63	110,30	2,01	43,95	90,13	896
W7	Groundwater	96	8,12	1228	103,70	296,57	11,18	74,42	112,38	2,41	39,61	59,32	725
W8	Groundwater	76	8,24	1975	342,82	423,92	28,84	121,54	107,80	1,71	97,67	134,12	1285
W9	Groundwater	29	8,33	1774	280,60	372,45	17,27	104,16	156,42	2,42	57,94	150,91	1169
W10	Groundwater	71	7,87	1388	323,30	251,57	24,35	60,83	127,24	1,61	52,93	92,36	966
W11	Groundwater	64	8,24	2910	275,72	705,78	9,82	179,66	376,90	3,59	57,36	131,49	1776
W12	Groundwater	92	8,34	1219	283,04	205,30	14,02	75,96	128,31	1,88	27,43	77,85	861
W13	Groundwater	45	8,02	1340	268,40	268,98	16,84	74,78	82,21	1,35	39,72	117,11	919
W14	Groundwater	87	8,91	1031	300,12	149,90	8,03	50,80	73,35	1,52	30,07	92,38	758
W15	Groundwater	92	8,6	802	217,16	77,28	3,92	71,78	47,55	1,73	25,07	71,80	552
W16	Groundwater	5	7,78	4000	429,44	981,18	9,85	349,54	554,20	12,61	119,73	208,05	2698
W17	Groundwater	71	8,50	1056	213,50	197,29	0,70	57,50	133,13	2,70	28,40	57,04	739
W18	Groundwater	87	8,34	1499	253,76	264,72	5,62	166,73	196,90	4,02	38,32	70,97	1043
W19	Groundwater	26	8,24	1085	246,44	160,86	1,45	128,04	72,84	1,50	53,82	88,07	806
W20	Groundwater	63	8,21	1953	305,00	310,42	1,86	317,90	288,06	6,30	54,19	92,55	1427
W21	Groundwater	26	8,5	1279	347,70	200,94	15,09	59,24	94,30	1,60	42,00	84,76	903
W23	Groundwater	21	8,79	772	307,44	44,83	50,88	29,07	25,28	22,74	35,84	69,59	772
W25	Groundwater	15	8,72	1894	620,98	150,62	38,24	287,71	173,76	5,62	114,78	82,59	1894
W26	Groundwater	17	8,65	1404	392,84	148,31		309,34	88,39	5,47	79,82	95,05	1404
W27	Groundwater	23	8,18	1938	347,70	385,86	30,60	117,63	116,30	2,76	60,99	186,34	1285
W28	Groundwater	23	8,72	2280	378,20	350,12	100,40	49,41	126,46	2,17	77,37	182,61	1331
W29	Groundwater	81	8,44	848	259,86	65,76	13,88	116,10	25,14	2,65	32,76	81,95	643
W30	Groundwater	47	8,39	1473	326,96	296,76	17,91	82,87	119,62	2,75	64,43	71,15	1022
W31	Groundwater	51	8,77	1539	229,36	333,77	31,83	41,57	101,58	2,39	52,67	98,52	929
W32	Groundwater	53	8,21	1491	253,76	287,61	18,92	84,84	135,04	1,88	44,45	66,18	924
W33	Groundwater	28	8,21	1745	326,96	329,40	20,17	129,31	189,52	2,30	59,07	97,42	1193
W34	Groundwater	63	8,87	1066	222,04	207,39	21,19	33,46	80,77	2,49	40,90	50,67	696
W35	Groundwater	24	7,76	1512	202,52	388,02	3,05	31,26	240,53	6,90	21,32	70,44	1014
W36	Groundwater	14	8,51	2070	519,72	221,68		253,91	280,79	1,94	59,12	97,69	1501
W41	Groundwater	35,3	8,5	874	317,20	76,17	23,29	53,96	44,77	1,20	47,87	67,87	657
W42	Groundwater	87	8,93	482	219,60	8,11	4,29	44,08	13,10	1,14	12,63	57,41	388
W43	Groundwater	61	8,53	1250	412,36	157,99	2,90	81,68	124,38	1,46	41,68	74,34	942
W44	Groundwater		8,34	575	200,08	39,72	14,14	52,16	60,70	1,05	24,15	25,23	474
W45	Groundwater	14	8,23	1245	268,40	262,61	5,16	41,05	141,70	3,98	22,41	63,01	831
W46	Groundwater	63	8,24	757	341,60	57,50	5,87	29,30	76,58	1,20	27,21	33,33	636
W47	Groundwater	27	8,37	1390	397,72	151,93	85,15	144,50	106,45	2,10	48,32	95,68	1089
W48	Groundwater	52	8,35	2380	351,36	167,00		658,24	177,98	3,08	57,87	267,60	1749
W49	Groundwater	40	8,29	2310	390,40	172,38	42,45	547,68	127,06	5,85	113,45	208,08	1652
W50	Groundwater	126	8,22	663	263,52	38,20	12,10	29,21	25,06	1,24	30,38	62,38	506
W51	Groundwater	27	8,33	1140	187,88	261,58	8,20	22,27	89,23	2,14	25,08	81,07	724
W52	Groundwater	67	8,11	922	351,36	95,87	6,89	42,35	84,64	1,45	20,82	79,52	747
W57	Groundwater		8,69	2890	274,50	735,23		101,78	460,84	6,41	46,02	120,27	1775
SP1	Springs		6,77	591	270,84	16,89	10,41	24,73	20,83	2,41	13,01	77,52	480
SP2	Springs		8,98	281	156,16	3,29		7,21	7,29	0,53	5,91	37,00	244
SP3	Springs		8,02	870	312,32	24,28	11,85	164,00	35,53	0,80	71,46	38,32	708

(*continued on next page*)

Table 1 (*continued*)

Number	Water type	Depth (m)	pH	CE25°C (µS/cm)	HCO_3^-	Cl^-	NO_3^-	SO_4^{2-}	Na^+	K^+	Mg^{2+}	Ca^{2+}	TDS
SP4	Springs		8,55	1921	375,76	200,39	26,31	406,63	100,20	3,33	106,86	178,62	1435
SP5	Springs		8,35	794	336,72	26,55	5,07	61,66	22,09	4,29	13,75	111,32	609
SP6	Springs		8,06	587	283,04	12,15	11,19	23,93	10,72	5,08	7,18	98,52	476
SP7	Springs		8,7	227	112,24	3,52	1,89	11,11	8,03	1,11	3,81	26,30	185
SP8	Springs		8,66	156,5	73,20	4,18	1,43	9,76	4,85	0,66	4,39	16,99	132
SP9	Springs		8,33	719	226,92	65,81	13,43	28,08	38,92	1,46	15,57	76,11	506
S1	Streamflow		9,58	455	223,26	17,46		17,68	20,11	1,96	9,70	51,89	179
S2	Streamflow		8,64	207	115,90	2,40	2,81	6,48	2,88	0,63	3,76	33,21	93
S3	Streamflow		8,5	581	294,02	16,45		21,76	19,66	2,29	11,61	72,59	235
S4	Streamflow		7,85	2120	225,70	522,96		47,16	261,02	8,42	37,56	128,78	181
S6	Streamflow		8,61	424	219,60	15,52		16,41	14,67	1,51	8,57	61,99	176
S7	Streamflow		8,56	794	331,84	17,50		78,06	19,38	3,50	14,39	117,91	265
S8	Streamflow		8,35	203	95,16	5,67		11,73	6,04	0,95	4,97	25,01	76
S9	Streamflow		8,76	97,1	36,60	2,73	1,61	7,72	3,80	0,54	2,91	8,01	29

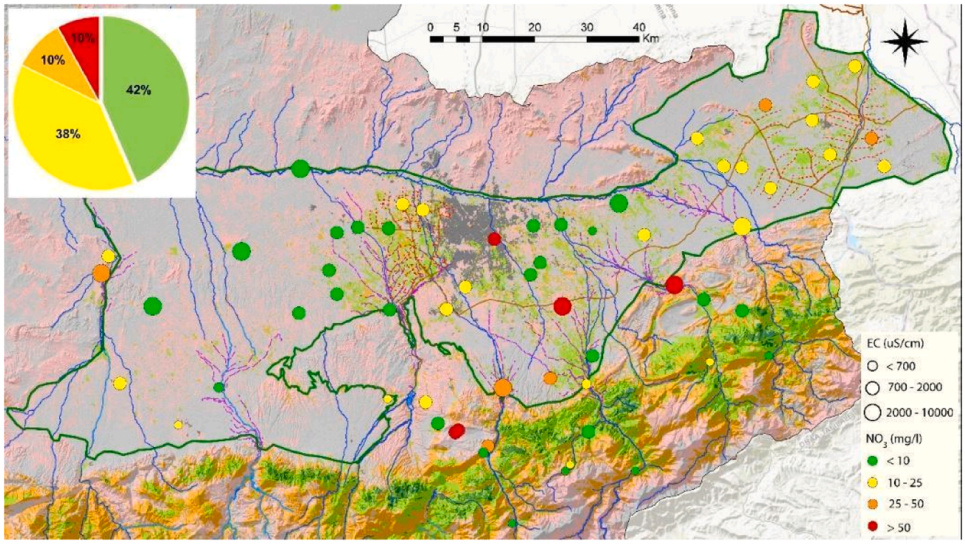

Fig. 4. Distribution of the salinity (electrical conductivity, EC) and nitrate in groundwater over the Haouz plain. The pie diagram presents the relative distribution of the nitrate classes.

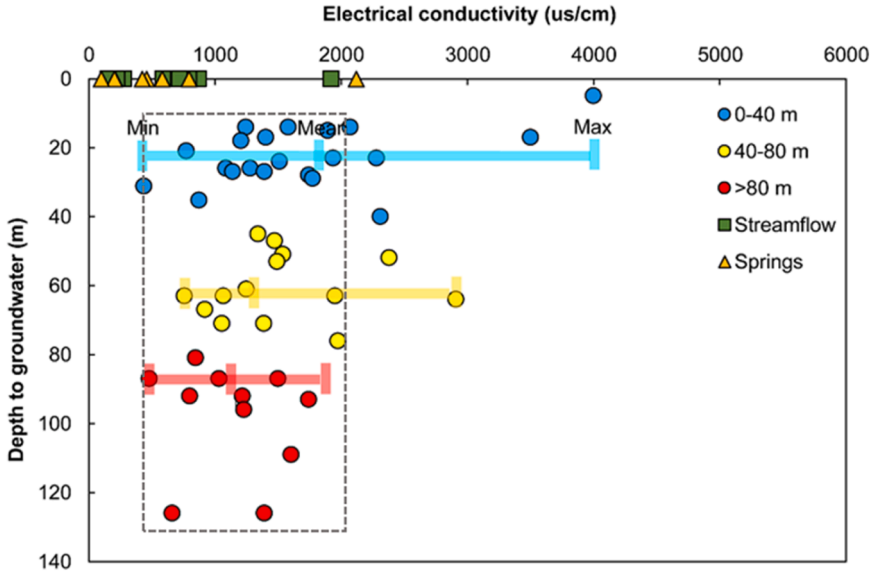

Fig. 5. Variation of electrical conductivity with depth to water table of the alluvial aquifer. The majority of measured groundwater (in the box) is slightly to moderately saline.

an increase of Cl^- concentrations with constant Na^+/Cl^-; they correspond to the 2 shallow wells W2 and W16 and to the deep well W11 (Fig. 7e). At lower salinities (lower Cl^- concentrations), a decline in $Na^+/Cl^- < 1$ indicates reverse ion exchange of Na^+ may also be influencing the groundwater chemistry (Fig. 7e). Evidence of reverse ion exchange, which consists of adsorption of groundwater Na^+ and release of Ca^{2+}-Mg^{2+} by the aquifer matrix, is also supported by the positive CAI-I and CAI-II (ion exchange indices) values of groundwater samples (Fig. 7f). Moreover, Fig. 7g illustrates the impact of anthropogenic activities on groundwater quality.

Rock weathering, halite dissolution, and reverse ion exchange affect groundwater at all depths. These processes are responsible for the initial geochemical features of the alluvial aquifer and are consistent with the basin geology (presence of silicate rocks, carbonate rocks and halite salt in the Triassic deposits). The similar geochemical facies observed in both shallow and deep groundwater may be attributed to the absence or weak stratification within the alluvial matrix of the aquifer, and to the common and temporally constant recharge sources, primarily from mountain waters as described in Section 2.1. Contamination by evaporates, specifically halite salt, could affect both shallow and deep groundwater. This is due to the presence of Triassic terrains and Paleozoic schists at the boundaries, both laterally and at the bottom of the alluvial aquifer.

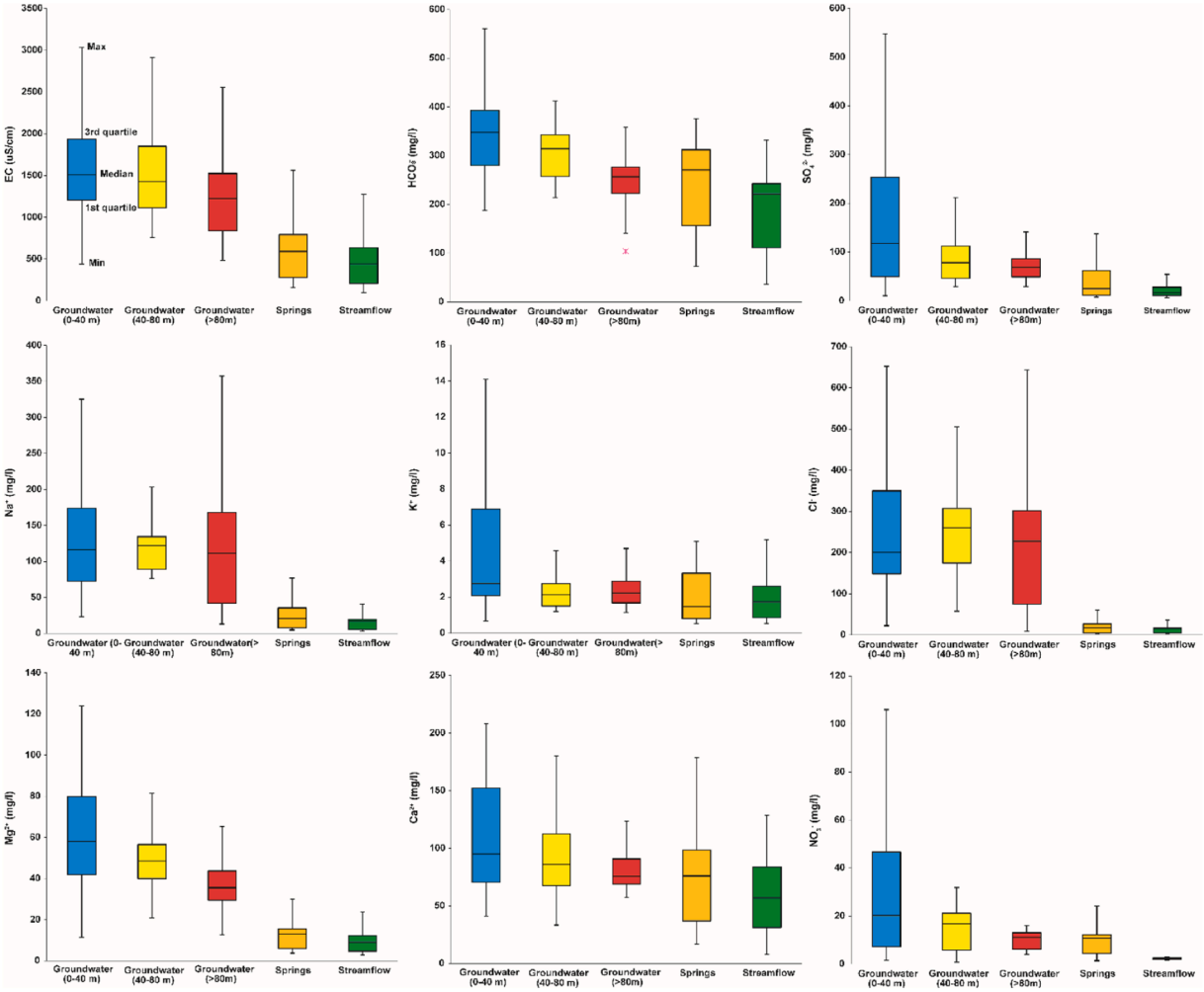

Fig. 6. Boxplots of EC, major ions and nitrate of groundwater at different depths (plain), and of springs and surface water (mountains). The colors indicate depths to the water table of the alluvial aquifer.

3.2. *Variation of groundwater nitrate*

The cumulative probability distribution of nitrate (NO_3^-) is shown on Fig. 8. The inflection point was estimated at 10 mg/l. The deduced values of the natural background level of nitrate (NBL-N) and of the anthropogenic nitrate level (APL-N) were 9.7 mg/l and 14 mg/l respectively. Studies have found similar or different values (e.g. Panno et al., 2006; Gemitzi, 2012; Rahman et al., 2021). In agricultural regions, those levels may be influenced by several parameters including naturally derived NO_2, soil organic matter from residue of fertilized and unfertilized crops, oxidizing environment in vadose zones and groundwaters (Huang et al., 2022), the size of the analyzed dataset and the sampling strategy (Panno et al., 2006).

In 2020, NO_3^- in groundwater across the plain ranges from a minimum of 0.7 mg/l to a max of 183 mg/l, with an average of 23 mg/l. Approximately 50 % of the groundwater samples have NO_3^- content exceeding the estimated APL-N of 14 mg/l, indicating anthropogenic contamination. About 10 % of the sampled wells exceed the limit of WHO drinking water guideline (50 mg/l). Up to 20 % exceed half this limit (25 mg/l) (Fig. 4), indicating clear trends towards harmful NO_3^- contents. Groundwater samples with NO_3^- exceeding 25 mg/l are primarily located near Marrakech city and beneath irrigated areas in the piedmont and in the East. As shown above (Fig. 7g), NO_3^- contamination could originate from agricultural activities or domestic sewage. The same contamination sources were suggested in the area by Boukhari et al. (2015) from a first analysis of the spatial distribution of nitrates. It is noteworthy that the contamination from the city of Marrakech is not addressed in sufficient detail in this study. An emphasis is needed around and beneath the city, as urbanization and industrialization may have significant impacts on the occurrence of NO_3^- (Zhang et al., 2020; Huang et al., 2018, 2022)

NO_3^- contamination is present in the groundwater at all depths. However, the variation of NO_3^- is much greater in the shallow groundwater than in deeper groundwater (Fig. 9). This confirms that the sources of NO_3^- contamination are from the land surface and that shallow groundwater is the most sensitive to surface contamination. Indeed, the relatively shallow groundwater (depths less than

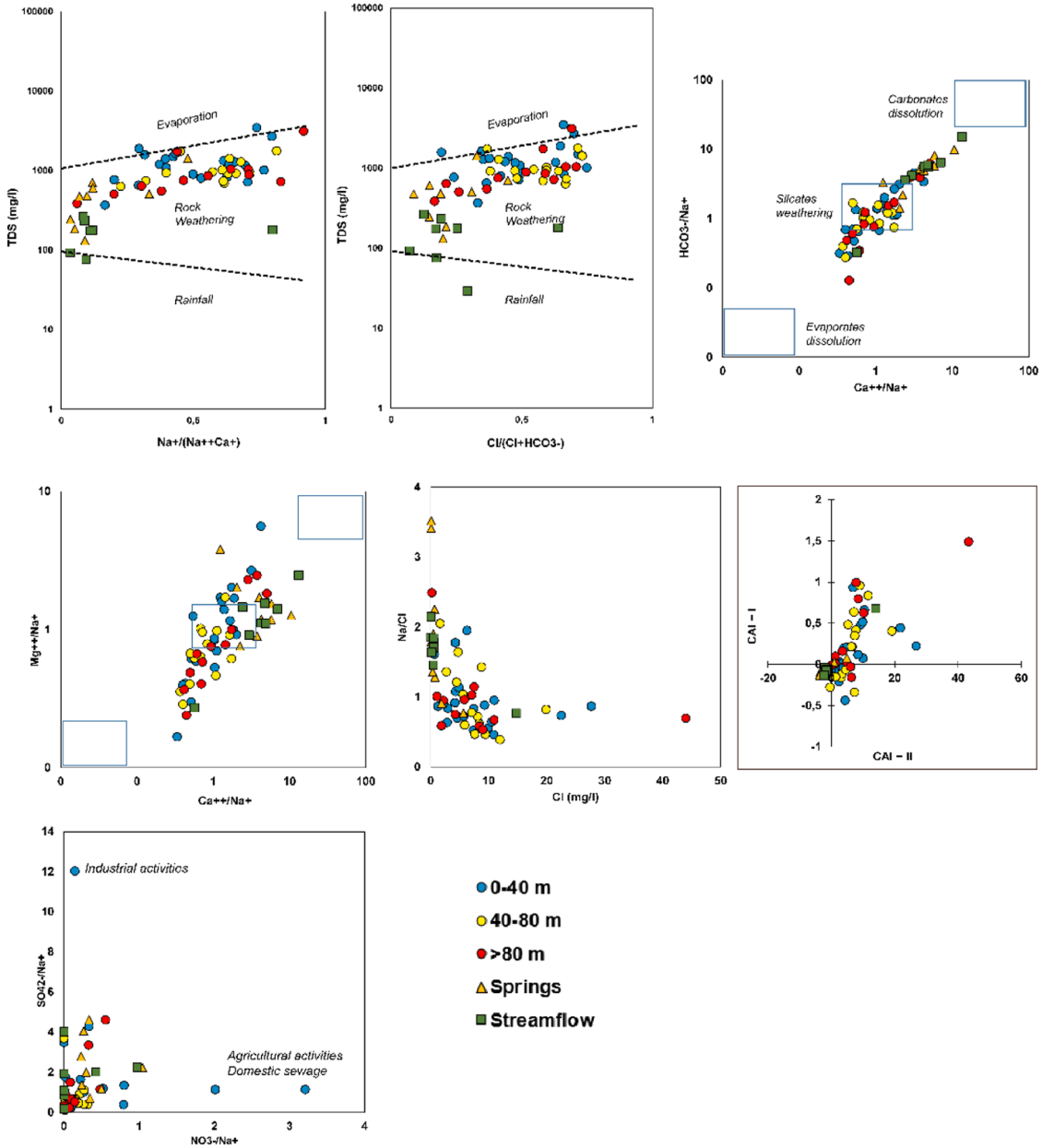

Fig. 7. (a) and (b) Gibbs plots, (c) Ca^{2+}/Na^{+} vs. $HCO_3^-/Na+$, (d) Ca^{2+}/Na^{+} vs. Mg^{2+}/Na^{+}, (e) Cl^- vs. Na^{+}/Cl^-, (f) CAI-1vs. CAI-2, (g) NO_3^-/Na^{+} vs. SO_4^{2-}/Na^{+}. The colors indicate depths to the water table of the alluvial aquifer.

40 m) has the highest values of NO_3^-, with an average of 37 mg/l and several values exceeding 50 mg/l. In deep groundwater (40–80 m depth), the average concentration of NO_3^- is 14.5 mg/l with a maximum of 42.5 mg/l, thus showing a central tendency to anthropogenic contamination. In very deep groundwater (80–130 m depth), the average concentration of NO_3^- is 9.8 mg/l, around the natural background concentration.

To determine whether the contamination is related to modern or ancient groundwater, we analyzed tritium (^3H) data collected alongside NO_3^- data (Fig. 9). A ^3H content greater than 2 tritium units (TU), as found in precipitation, indicates modern surface water or groundwater. A ^3H content of less than 1 TU indicates a greater contribution of pre-1960s water, and thus pre-modern water that has a longer residence time (Clark and Fritz, 1997). ^3H was not measured for all the samples. According to the available values, the relatively shallow groundwater (20–40 m depth) in the alluvial aquifer shows the most significant contribution of modern groundwater, as the ^3H activity varies between 0.40 TU and 3.30 TU, with an average of 1.54 TU (Fig. 9). It also has the highest NO_3^- concentrations. Deeper groundwater (> 40 m) exhibits on average lower tritium activity, the mean value is 0.49 TU at depths ranging from 40 to 80 m and 0.98 TU at depths greater than 80 m. Three deep groundwater samples present ^3H values of modern groundwater: W5 (109 m, 1.9 TU,

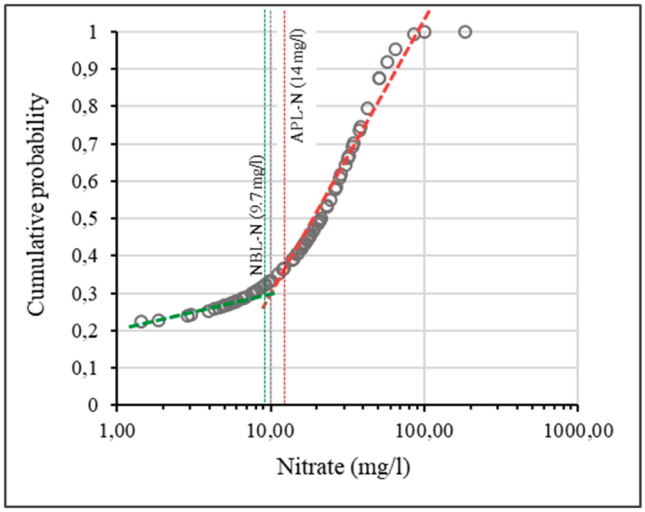

Fig. 8. Cumulative probability plots of the nitrate (NO_3^-) concentration in the alluvial aquifer of the Haouz plain. NBL-N is the estimated natural background level of nitrate, and APL-N is the anthropogenic nitrate level.

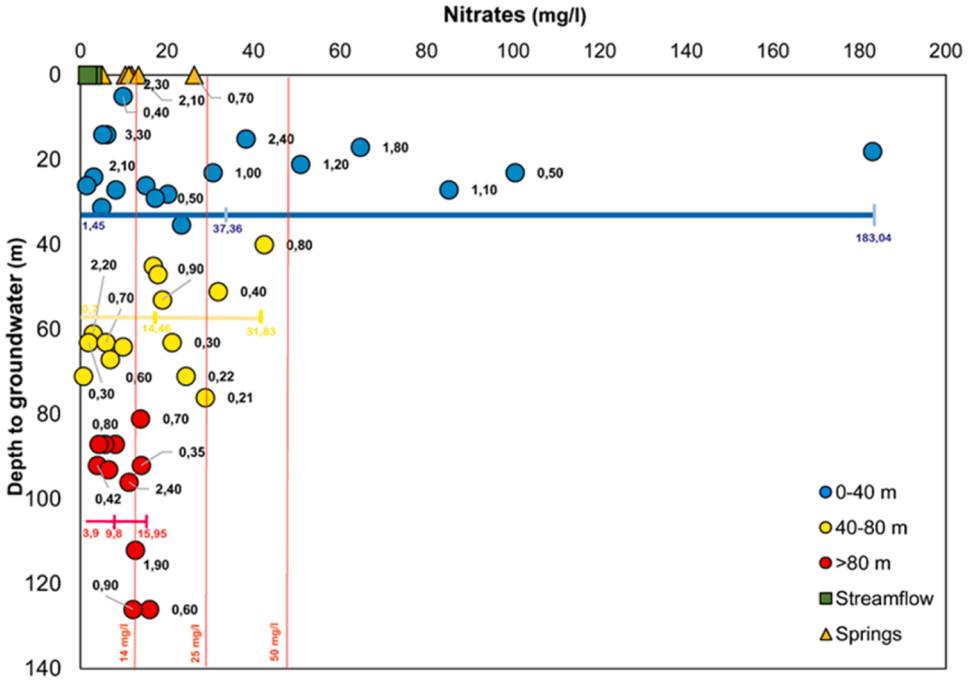

Fig. 9. Variation of nitrate with depth to the water table of the alluvial aquifer. The numbers represent measured tritium activity in UT. The nitrate thresholds represent the WHO drinking water guideline (≥ 50 mg/l), half of this value (25 mg/l) and the estimated anthropogenic nitrate level (14 mg/l).

12.3 mg/l NO_3^-), W7 (96 m, 2.4 TU, 11.2 mg/l NO_3^-) and W43 (61 m, 2.2 TU, 3 mg/l NO_3^-). The variability in ^3H levels suggests different contamination processes, some may be linked to the effects of groundwater depletion as discussed in the following section.

3.3. Effects of the groundwater depletion on nitrate and salinity

Due to groundwater depletion, over 65 % of our alluvial aquifer currently has depth to water table greater than 40 m, and it reaches more than 100 m in some sectors. Shallow groundwater is disappearing and wells are increasingly tapping deep levels. The remaining shallow groundwater (< 40 m) is the most affected by NO_3^-, with an average of 37 mg/l and up to 61 % of the measured shallow wells are contaminated according to the estimated anthropogenic nitrate level (14 mg/l). Furthermore, it is the most enriched in ^3H (1.54 TU

on average), which indicates recent infiltrations of elevated NO_3^-. Deeper groundwater (40 m - 130 m) is less contaminated by NO_3^- with an average of 13.5 mg/l. Nevertheless, about 40 % of deep wells exceeds the anthropogenic nitrate level. According to ^3H data, the majority of the contaminated deep groundwater has less than 1 TU. This suggests long residence times of NO_3^- in the aquifer, which could be related to historical use of fertilizers as the agricultural activities in the plain are ancient. More likely, it could result from dual porosity, where infiltrating younger groundwater carrying high loads of NO_3^- mixes with inflowing older deep groundwater that has low nitrate content. Evidence of the mobilization of modern groundwater to deep levels in the aquifer is given by the existence of deep groundwater with concentration of ^3H around 2 TU. The transport of modern shallow groundwater to high depths in the aquifer might be the result of preferential flow pathways, which allow fast flow from the surface to deep levels. Naturally occurring fast flows are known into carbonate aquifers as focused recharge (Hartmann et al., 2021). In our aquifer, formed of alluvial lithology and porous texture, focused recharge may occur only as stream losses in the piedmont where the water-table is still relatively shallow (Fakir et al., 2021). Deep groundwater in the Haouz plain is currently extended in the areas where the irrigation pumping is intense, resulting in high rates of depletion. In this context, the transport of shallow groundwater to deep levels within the aquifer may be particularly favoured by the effects of downward groundwater movement due to intensive pumping, which may result in the redistribution of groundwater within the aquifer. Indeed, using numerical modeling and groundwater age tracing, several studies (Kagabu et al., 2013; Taufiq et al., 2018) have stated that vertical flow becomes dominant in aquifers under intensive pumping, allowing modern shallow groundwater to reach deeper depths and mix with deep and older groundwater, a phenomenon called rejuvenation. Consequently, where shallow groundwater is contaminated, these processes have the potential to threaten the quality of deep groundwater, especially for chemical contaminants with high water solubility and mobility, such as nitrate (Burow et al., 2007; Lapworth et al., 2017).

Furthermore, it was observed that the majority of the pumped groundwater in our study is slightly (EC $<$ 700 μS/cm) to moderately (EC $<$ 2000 μS/cm) saline, and its NO_3^- content remains moderately elevated (23 mg/l on average). These characteristics appear paradoxical when considered in the context of the arid climate and the high level of anthropogenic activity in the plain. Those conditions normally lead to higher salinity and nitrate values as measured in other (semi)arid plains in Morocco (e.g., Benkaddour et al., 2020; El Ghali et al., 2020; Elmeknassi et al., 2022) and in the Mediterranean region (e.g., Mas-Pla and Menció, 2019; Menció et al., 2016; Re et al., 2017; Abascal et al., 2022). Indeed, the natural and anthropogenic threats to groundwater quality cannot be ignored in the Haouz plain. The potential factors are the high evapotranspiration (1600 mm), the intensively growing irrigated agricultural activities (Ouassanouan et al., 2022) and the poor sanitation in the rural and peri-urban agglomerations, which mainly rely on septic tanks and the release of raw wastewater into the environment (UNICEF, 2019; Dahbi and Messaoudi, 2020). The harmful NO_3^- levels (50–183 mg/l) measured locally in the relatively shallow groundwater confirm the effective impact of these threats. The moderate levels of salinity and nitrate in our aquifer are due to the large extent of deep groundwater of good quality and the disappearance of shallow groundwater that is more sensitive to the effects of evapotranspiration (Shah et al., 2007) and to NO_3^- contamination (Eccles and Bradford, 1976; Spalding and Exner, 1993; MacLeod et al., 1995).

The occurrence of shallow groundwater is currently very limited because of the high decline in the water table resulting from depletion. The developed thick unsaturated zone could also mitigate surface-borne contamination because of the generally long transit time (of years or decades or much longer) of chemicals (McMahon et al., 2006). However, thick unsaturated zone that appears currently beneficial for the protection of groundwater against surface contamination, may release further contaminants in deep groundwater after sufficient migration time or at future increases in groundwater recharge rates associated with climate or land use changes (Riedel and Weber, 2020). Managed aquifer recharge (MAR) is a remediation measure frequently recommended in arid and semiarid regions as a management action to enhance groundwater recovery (Al-Ruzouq et al., 2019; Markovich et al., 2019). Indeed, water managers in our basin have invested in MAR projects in several wadis (Fakir and Bouimouass, 2019). It is imperative that future planning of MAR projects must take into account the potential leaching of nitrate accumulated in the unsaturated zone, through appropriate selection of sites and techniques for MAR.

4. Conclusion

The present study investigated the salinity and nitrate in groundwater beneath a highly developed arid plain, where the alluvial unconfined aquifer is currently experiencing a severe depletion. Consequently, shallow groundwater has been disappearing while deep groundwater has been increasingly pumped for irrigation. It was found that the dominant hydrochemical characteristics of the groundwater are controlled by rock weathering processes of silicates and carbonates, dissolution of halite in the Triassic deposits, and reverse ion exchange. Several features linked to the depletion were highlighted. Concerning the salinity, the declining water-table may have reduced the salinization of groundwater by evaporation (and transpiration) effects. However, tapping deep levels of the aquifer increases the risk of pumping deep saline groundwater, which is contaminated by leaching from Triassic deposits and Paleozoic schists at the bottom of alluvial aquifer. Concerning the nitrate, according to the estimated anthropogenic level (14 mg/l), the contamination affects both shallow and deep groundwater. In shallow groundwater, the levels of contamination are much greater than in the deep groundwater, confirming the high sensitivity of shallow groundwater to surface contamination. The high tritium content of shallow groundwater attested that recent infiltration of elevated NO_3^- water is the main contamination process. In deep groundwater, nitrate could originate from old sources related to historical use of fertilizers as the agricultural activities in the plain are ancient. In the current context of intensive groundwater pumping, shallow nitrate-rich groundwater can be transported to deeper levels within the aquifer by vertical induced flows.

In addition, the induced thick unsaturated zone in depleted aquifers may accumulate surface-borne nitrate and other contaminants. Consequently, future contamination issues may emerge after sufficient migration time for contaminants, or after changes in the recharge regime due to climate or land use changes, or when the water table rises due to replenishment measures. Thus, the main

quantitative features that characterize the aquifers under depletion: intensive pumping regime, decline of the water table, thickening of the unsaturated zone, would complicate or exacerbate the groundwater contamination processes. Therefore, further studies and field experiments on contaminant transport through thickening unsaturated zones are needed. Addressing both depletion and contamination is crucial to protecting groundwater and improving its long-term sustainability.

CRediT authorship contribution statement

Abdelghani Chehbouni: Writing – review & editing, Validation. **Rabia Benaddi:** Data curation. **Hamza Sahraoui:** Writing – original draft, Methodology, Investigation. **Younes Fakir:** Writing – review & editing, Writing – original draft, Methodology, Conceptualization. **Sarah Tweed:** Writing – original draft, Validation. **Houssne Bouimouass:** Writing – original draft, Conceptualization. **Marc Leblanc:** Writing – review & editing, Validation.

Declaration of Competing Interest

The authors declare that they have no known competing financial interests or personal relationships that could have appeared to influence the work reported in this paper.

Acknowledgements

We would like to thank several institutions and projects for their collaboration and support. Field measurement campaigns were carried out in the framework of SAGESSE project (PPR-B/2015/48) and with the support of Geosciences Semlalia laboratory of Cadi Ayyad University (Marrakech, Morocco). The Hydrogeology Laboratory, UMR EMMAH, University of Avignon (Avignon, France), performed the geochemical analyses. The Tensift Hydraulic Basin Agency (ABHT, Marrakech, Morocco) provided some groundwater data. Additional support came from PRIMA-S2 ALTOS project, PRIMA-IDEWA project, GEANTech project (the APRD research program), the Center of Remote Sensing Applications, CRSA, UM6P (Benguerir, Morocco).

Data Availability

Data will be made available on request.

References

Abascal, E., Gómez-Coma, L., Ortiz, I., Ortiz, A., 2022. Global diagnosis of nitrate pollution in groundwater and review of removal technologies. Sci. Total Environ., 152233 https://doi.org/10.1016/j.scitotenv.2021.152233.

Abuelgasim, A., Ammad, R., 2018. Mapping soil salinity in arid and semi-arid regions using Landsat 8 OLI satellite data. Remote Sens. Appl. Soc. Environ. https://doi.org/10.1016/j.rsase.2018.12.010.

Ait Lemkademe, A., Michelot, J.L., Benkaddour, A., Hanich, L., Heddoun, O., 2022. Origin of groundwater salinity in the draa Sfar polymetallic mine area using conservative elements (Morocco). Water 15 (1), 82.

Al-Ruzouq, R., Shanableh, A., Merabtene, T., Siddique, M., Khalil, M.A., Idris, A., Almulla, E., 2019. Potential groundwater zone mapping based on geo-hydrological considerations and multi-criteria spatial analysis: North UAE. Catena 173, 511–524.

Andreu, J.M., Pulido-Bosch, A., Llamas, M.R., Bru, C., Martinez-Santos, P., Garcia-Sanchez, E., Villacampa, L., 2008. Overexploitation and water quality in the Crevillente aquifer (Alicante, SE Spain). In: Prats-Rico, D., Brebbia, C.A., Villacampa-Esteve, Y. (Eds.), Water pollution IX, WIT Transactions on Ecology and the Environment. WIT Press, Southampton, pp. 75–84. https://doi.org/10.2495/WP080081.

Aureli, A., Ganoulis, J., Margat, J., 2008. Groundwater resources in the mediterranean region: importance, uses and sharing. Water Mediterr. 96–105.

Badaruddin, S., Werner, A.D., Morgan, L.K., 2015. Water tablesalinization due to seawater intrusion. Water Resour. Res. 51, 8397–8408. https://doi.org/10.1002/2015WR017098.

Baillieux, A., Campisi, D., Jammet, N., Bucher, S., Hunkeler, D., 2014. Regional water quality patterns in an alluvial aquifer: direct and indirect influences of rivers. J. Contam. Hydrol. 169, 123–131. https://doi.org/10.1016/j.jconhyd.2014.09.002.

Benkabbour, B., Toto, E.A., Fakir, Y., 2004. Using DC resistivity method to characterize the geometry and the salinity of the Plioquaternary consolidated coastal aquifer of the Mamora plain, Morocco. Env Geol. 45, 518–526. https://doi.org/10.1007/s00254-003-0906-y.

Benkaddour, R., Merimi, I., Szumiata, T., Hammouti, B., 2020. Nitrates in the groundwater of the Triffa plain eastern Morocco. Mater. Today Proc. (2020). https://doi.org/10.1016/j.matpr.2020.04.120.

Bernet, G., Prost, J.P., 1975. Le Haouz de Marrakech et le bassin du Mejjate; in Ressources en eau du Maroc - Tome 2. Notes et Mémoires du Service Géologique, 231, Rabat, Morocco.

Bhatnagar, A., Sillanpää, M., 2011. A review of emerging adsorbents for nitrate removal from water. Chem. Eng. J. 168 (2), 493–504.

Blarasin, M., Cabrera, A., Matiatos, I., Quinodóz, F.B., Albo, J.G., Lutri, V., Matteoda, E., Panarello, H., 2020. Comparative evaluation of urban versus agricultural nitrate sources and sinks in an unconfined aquifer by isotopic and multivariate analyses. Sci. Total Environ. 741. https://doi.org/10.1016/j.scitotenv.2020.140374.

Bouimouass, H., Fakir, Y., Tweed, S., Leblanc, M., 2020. Groundwater recharge sources in semiarid irrigated mountain fronts. Hydrol. Process. 34 (7), 1598–1615.

Bouimouass, H., Tweed, S., Marc, V., Fakir, Y., Sahraoui, H., Leblanc, M., 2024. The importance of mountain-block recharge in semiarid basins: an insight from the High-Atlas, Morocco. J. Hydrol. 631. https://doi.org/10.1016/j.jhydrol.2024.130818.

Boukhari, K., Fakir, Y., Stigter, T.Y., et al., 2015. Origin of recharge and salinity and their role on management issues of a large alluvial aquifer system in the semi-arid Haouz plain, Morocco. Environ. Earth Sci. 73, 6195–6212. https://doi.org/10.1007/s12665-014-3844-y.

Burow, K.R., Dubrovsky, N.M., Shelton, J.L., 2007. Temporal trends in concentrations of DBCP and nitrate in groundwater in the eastern San Joaquin Valley, California, USA. Hydrogeol. J. 15, 991–1007. https://doi.org/10.1007/s10040-006-0148-7.

Clark, I.D., Fritz, P., 1997. Environmental Isotopes in Hydrogeology. CRC press.

Dahbi, N., Messaoudi, L., 2020. Epidemiological profile of patients with waterborne diseases in the cities of Meknes and Khemisset (Morocco). Int. J. Innov. Appl. Stud. 29 (1), 59–64. ISSN 2028-9324.

Eccles, L.A., Bradford, W.L., 1976. Distribution of nitrate in ground water, Redlands, California. U.S. Geological Survey Water-Resources Investigations Report 76-117, 38 p.

El Ghali, T., Marah, H., Qurtobi, M., Raibi, F., Bellarbi, M., Amenzou, N., El Mansouri, B., 2020. Geochemical and isotopic characterization of groundwater and identification of hydrogeochemical processes in the Berrechid aquifer of Central Morocco. Carbonates Evaporites 35 (2020), 1–21. https://doi.org/10.1007/s13146-020-00571-y.

Elmeknassi, M., Bouchaou, L., El Mandour, A., Elgettafi, M., Himi, M., Casas, A., 2022. Multiple stable isotopes and geochemical approaches to elucidate groundwater salinity and contamination in the critical coastal zone: a case from the Bou-areg and Gareb aquifers (North-Eastern Morocco). Environ. Pollut. 300, 118942.

Fakir, Y., Bouimouass, H., Constantz, J., 2021. Seasonality in intermittent streamflow losses beneath a semiarid Mediterranean Wadi. Water Resour. Res. 57 (6), e2021WR029743.

Fakir, Y., Bouimouass, H., 2019. Insights from groundwater level measurements over a managed aquifer recharge site in Central Morocco. In Proceedings of the International Symposium on Managed Aquifer Recharge (pp. 153-160).

Fishman, R.M., Siegfried, T., Raj, P., Modi, V., Lall, U., 2011. Over-extraction from shallow bedrock versus deep alluvial aquifers: reliability versus sustainability considerations for India's groundwater irrigation. Water Resour. Res. 47 (6).

Gan, L., Huang, G., Pei, L., Gan, Y., Liu, C., Yang, M., Han, D., Song, J., 2022. Distributions, origins, and health-risk assessment of nitrate in groundwater in typical alluvial-pluvial fans, North China Plain. Environ. Sci. Pollut. Res. 29, 17031–17048. https://doi.org/10.1007/s11356-021-17067-4.

Gemitzi, A., 2012. Evaluating the anthropogenic impacts on groundwaters; a methodology based on the determination of natural background levels and threshold values. Environ. Earth Sci. 67, 2223–2237. https://doi.org/10.1007/s12665-012-1664-5.

Gerten, D., Hoff, H., Rockström, J., Jägermeyr, J., Kummu, M., Pastor, A.V., 2013. Towards a revised planetary boundary for consumptive freshwater use: role of environmental flow requirements. Curr. Opin. Environ. Sustain. 5 (6), 551–558.

Ghalib, H.B., 2017. Groundwater chemistry evaluation for drinking and irrigation utilities in east Wasit province, Central Iraq. Appl. Water Sci. 7, 3447–3467. https://doi.org/10.1007/s13201-017-0575-8.

Gowing, J.W., Rose, D.A., Ghamarnia, H., 2009. The effect of salinity on water productivity of wheat under deficit irrigation above shallow groundwater. Agric. Water Manag. 96 (3), 517–524.

Gu, B.J., Ge, Y., Chang, S.X., Luo, W.D., Chang, J., 2013. Nitrate in groundwater of China: sources and driving forces. Glob. Environ. Chang 23 (5), 1112–1121. https://doi.org/10.1016/j.gloenvcha.2013.05.004.

Hajhouji, Y., Fakir, Y., Gascoin, S., Simonneaux, V., Chehbouni, A., 2022. Dynamics of groundwater recharge near a semi-arid Mediterranean intermittent stream under wet and normal climate conditions. J. Arid Land 14 (7), 739–752.

Hartmann, A., Jasechko, S., Gleeson, T., Wada, Y., Andreo, B., Barberá, J.A., Brielmann, H., Bouchaou, L., Charlier, J., Darling, G., Filippini, M., Garvelmann, J., Goldscheider, N., Kralik, M., Kunstmann, H., Ladouche, B., Lange, J., Lucianetti, G., Martín, G.F., Mudarra, M., Sánchez, D., Stumpp, C., Zagana, E., Wagener, T., 2021. Risk of groundwater contamination widely underestimated because of fast flow into aquifers. PNAS 118. https://doi.org/10.1073/pnas.2024492118.

Huang, G., Liu, C., Sun, J., Zhang, M., Jing, J., Li, L., 2018. A regional scale investigation on factors controlling the groundwater chemistry of various aquifers in a rapidly urbanized area: a case study of the Pearl River Delta. Sci. Total Environ. 625. https://doi.org/10.1016/j.scitotenv.2017.12.322.

Huang, G., Pei, L., Li, L., Liu, C., 2022. Natural background levels in groundwater in the Pearl River Delta after the rapid expansion of urbanization: a new pre-selection method. Sci. Total Environ. 813. https://doi.org/10.1016/j.scitotenv.2021.151890.

Kagabu, M., Shimada, J., Delinom, R., Nakamura, T., Taniguchi, M., 2013. Groundwater age rejuvenation caused by excessive urban pumping in Jakarta area, Indonesia. Hydrol. Process. 27, 2591–2604. https://doi.org/10.1002/hyp.9380.

Kamal, S., Sefiani, S., Laftouhi, N.E., El Mandour, A., Moustadraf, J., Elgettafi, M., Casas, A., 2021. Hydrochemical and isotopic assessment for characterizing groundwater quality and recharge processes under a semi-arid area: case of the Haouz plain aquifer (Central Morocco). J. Afr. Earth Sci. 174, 104077.

Kapembo, M.L., Laffite, A., Bokolo, M.K., Mbanga, A.L., Maya-Vangua, M.M., Otamonga, J.P., Poté, J., 2016. Evaluation of water quality from suburban shallow wells under tropical conditions according to the seasonal variation, Bumbu, Kinshasa, Democratic Republic of the Congo. Expo. Health 8 (4), 487–496.

Konikow, Leonard F., 2015. Long-term groundwater depletion in the United States. Groundwater 53, 2–9. https://doi.org/10.1111/gwat.12306.

Kummu, M., Guillaume, J.H.A., de Moel, H., Eisner, S., Flörke, M., Porkka, M., Siebert, S., Veldkamp, T.I.E., Ward, P.J., 2016. The world's road to water scarcity: shortage and stress in the 20th century and pathways towards sustainability. Sci. Rep. 6 (1). https://doi.org/10.1038/srep38495.

Lapworth, D.J., Krishan, G., MacDonald, A.M., Rao, M.S., 2017. Groundwater quality in the alluvial aquifer system of northwest India: new evidence of the extent of anthropogenic and geogenic contamination. Sci. Total Environ. 599–600. https://doi.org/10.1016/j.scitotenv.2017.04.223.

Liu, R., Xie, X., Hou, Q., Han, D., Song, J., Huang, G., 2024. Spatial distribution, sources, and human health risk assessment of elevated nitrate levels in groundwater of an agriculture-dominant coastal area in Hainan Island, China. J. Hydrol. 634. https://doi.org/10.1016/j.jhydrol.2024.131088.

MacLeod, C.L., Barringer, T.H., Vowinkel, E.F., Price, C.V. (1995). Relation of Nitrate Concentrations in Ground Water to Well Depth, Well Use, and Land Use in Franklin Township, Gloucester County, New Jersey, 1970-85. U.S. GEOLOGICAL SURVEY Water-Resources Investigations Report 94-4174.

Manu, E., Afrifa, G.Y., Ansah-Narh, T., Sam, F., Akosua Loh, Y.S., 2022. Estimation of natural background and source identification of nitrate-nitrogen in groundwater in parts of the Bono, Ahafo and Bono East regions of Ghana. Groundw. Sustain. Dev. 16. https://doi.org/10.1016/j.gsd.2021.100696.

Margat, J., Van der Gun, J., 2013. Groundwater Around the World: A Geographic Synopsis. Crc Press.

Markovich, K.H., Manning, A.H., Condon, L.E., McIntosh, J.C., 2019. Mountain-block recharge: a review of current understanding. Water Resour. Res. 55 (11), 8278–8304.

Marston, L., Konar, M., Cai, X., Troy, T.J., 2015. Virtual groundwater transfers from overexploited aquifers in the United States. Proc. Natl. Acad. Sci. 112 (28), 8561–8566.

Mas-Pla, J., Menció, A., 2019. Groundwater nitrate pollution and climate change: learnings from a water balance-based analysis of several aquifers in a western Mediterranean region (Catalonia). Environ. Sci. Pollut. Res Int 26 (3), 2184–2202. https://doi.org/10.1007/s11356-018-1859-8.

McMahon, P.B., Dennehy, K.F., Bruce, B.W., Bo hlke, J.K., Michel, R.L., Gurdak, J.J., Hurlbut, D.B., 2006. Storage and transit time of chemicals in thick unsaturated zones under rangeland and irrigated cropland, High Plains, United States. Water Resour. Res. 42, W03413. https://doi.org/10.1029/2005WR004417.

Menció, A., Mas-Pla, J., Otero, N., Regàs, O., Boy-Roura, M., Puig, R., Folch, A., 2016. Nitrate pollution of groundwater; all right…, but nothing else? Sci. Total Environ. 539, 241–251. https://doi.org/10.1016/j.scitotenv.2015.08.151.

Mukherjee, A., Saha, D., Harvey, C.F., Taylor, R.G., Ahmed, K.M., Bhanja, S.N., 2015. Groundwater systems of the Indian Sub-Continent. J. Hydrol. Reg. Stud. 4. https://doi.org/10.1016/j.ejrh.2015.03.005.

Ouassanouan, Y., Fakir, Y., Simonneaux, V., Kharrou, M.H., Bouimouass, H., Najar, I., Chehbouni, A., 2022. Multi-decadal analysis of water resources and agricultural change in a Mediterranean semiarid irrigated piedmont under water scarcity and human interaction. Sci. Total Environ. 834, 155328.

Panno, S.V., Kelly, W.R., Martinsek, A.T., Hackley, K.C., 2006. Estimating background and threshold nitrate concentrations using probability graphs. Ground Water 44 (5), 697–709. https://doi.org/10.1111/j.1745-6584.2006.00240.x.

Perrone, D., Jasechko, S., 2019. Deeper well drilling an unsustainable stopgap to groundwater depletion. Nat. Sustain. 2 (8), 773–782.

Prusty, P., Farooq, S.H., 2020. Seawater intrusion in the coastal aquifers of India - a review. HydroResearch 3, 61–74. https://doi.org/10.1016/j.hydres.2020.06.001.

Puig, R., Soler, A., Widory, D., Mas-Pla, J., Domènech, C., Otero, N., 2017. Characterizing sources and natural attenuation of nitrate contamination in the BaixTer aquifer system (NE Spain) using a multi-isotope approach. Sci. Total Environ. 580, 518–532. https://doi.org/10.1016/j.scitotenv.2016.11.206.

Rahman, A., Mondal, N.C., Tiwari, K.K., 2021. Anthropogenic nitrate in groundwater and its health risks in the view of background concentration in a semi arid area of Rajasthan, India. Sci. Rep. 11, 9279. https://doi.org/10.1038/s41598-021-88600-1.

Rajmohan, N., Masoud, M.H.Z., Niyazi, B.A.M., 2021. Impact of evaporation on groundwater salinity in the arid coastal aquifer, Western Saudi Arabia. CATENA 196. https://doi.org/10.1016/j.catena.2020.104864.

Re, V., Sacchi, E., Kammoun, S., Tringali, C., Trabelsi, R., Zouari, K., Daniele, S., 2017. Integrated socio-hydrogeological approach to tackle nitrate contamination in groundwater resources. The case of Grombalia Basin (Tunisia). Sci. Total Environ. 593–594, 664–676. https://doi.org/10.1016/j.scitotenv.2017.03.151.

Rhoades, J.D., Kandiah, A., Mashali, A.M. (1992). The Use of Saline Waters for Crop Production-FAO 806 Irrigation and Drainage, paper 48. FAO, Rome, 133.

Riedel, T., Weber, T.K.D., 2020. Review: The influence of global change on Europe's water cycle and groundwater recharge. Hydrogeol. J. 28, 1939–1959. https://doi.org/10.1007/s10040-020-02165-3.

Rodriguez-Estrella, T., 2014. The problems of overexploitation of aquifers in semi-arid areas: characteristics and proposals for mitigation. Boletin Geol. Y. Min. 125, 91–109. https://doi.org/10.5194/hessd-9-5729-2012.

Rosa, L., Rulli, M.C., Davis, K.F., Chiarelli, D.D., Passera, C., D'Odorico, P., 2018. Closing the yield gap while ensuring water sustainability. Environ. Res. Lett. 13 (10), 104002.

Salameh, E., Hammouri, R., 2008. Sources of groundwater salinity along the flow path, Disi–Dead Sea/Jordan. Environ. Geol. 55, 1039–1053. https://doi.org/10.1007/s00254-007-1053-7.

Shah, N., Nachabe, M., Ross, M., 2007. Extinction depth and evapotranspiration from ground water under selected land covers. Ground Water 45 (3). https://doi.org/10.1111/j.1745-6584.2007.00302.x.

Singh, A., 2019. An overview of drainage and salinization problems of irrigated lands. Irrig. Drainage 68. https://doi.org/10.1002/ird.2344.

Soleimani, H., Nasri, O., Ghoochani, M., Azhdarpoor, A., Dehghani, M., Radfard, M., Heydari, M., 2020. Groundwater quality evaluation and risk assessment of nitrate using monte carlo simulation and sensitivity analysis in rural areas of Divandarreh County, Kurdistan province, Iran. Int. J. Environ. Anal. Chem. 102 (10), 2213–2231. https://doi.org/10.1080/03067319.2020.1751147.

Spalding, R.F., Exner, M.E., 1993. Occurrence of nitrate in groundwater-a review. J. Environ. Qual. 22, 392–402.

Subba Rao, N., Sunitha, B., Adimalla, N., Chaudhary, M., 2020. Quality criteria for groundwater use from a rural part of Wanaparthy District, Telangana State, India, through ionic spatial distribution (ISD), entropy water quality index (EWQI) and principal component analysis (PCA). Environ. Geochem. Health 42, 579–599.

Taufiq, A., Hosono, T., Ide, K., et al., 2018. Impact of excessive groundwater pumping on rejuvenation processes in the Bandung basin (Indonesia) as determined by hydrogeochemistry and modeling. Hydrogeol. J. 26, 1263–1279. https://doi.org/10.1007/s10040-017-1696-8.

UNICEF (2019). MOROCCO Water, Sanitation and Hygiene. Sectoral and OR+ Thematic Report.

Wada, Y., Bierkens, M.F., 2014. Sustainability of global water use: past reconstruction and future projections. Environ. Res. Lett. 9 (10), 104003.

Wada, Y., Van Beek, L.P., Van Kempen, C.M., Reckman, J.W., Vasak, S., Bierkens, M.F., 2010. Global depletion of groundwater resources. Geophys. Res. Lett. 37 (20).

Wang, D., Zhao, C., Zheng, J., Zhu, J., Gui, Z., Yu, Z., 2021. Evolution of soil salinity and the critical ratio of drainage to irrigation (CRDI) in the Weigan Oasis in the Tarim Basin. CATENA 201. https://doi.org/10.1016/j.catena.2021.105210.

Werner, A.D., 2017. On the classification of seawater intrusion. J. Hydrol. 551. https://doi.org/10.1016/j.jhydrol.2016.12.012.

WHO, 2004. Rolling Revision of the WHO Guidelines for Drinking-water Quality. World Health Organization, Geneva.

Xanke, J., Liesch, T., 2022. Quantification and possible causes of declining groundwater resources in the Euro-Mediterranean region from 2003 to 2020. Hydrogeol. J. 30, 379–400. https://doi.org/10.1007/s10040-021-02448-3.

Yu, G., Wang, J., Liu, L., Li, Y., Zhang, Y., Wang, S., 2020. The analysis of groundwater nitrate pollution and health risk assessment in rural areas of Yantai, China. BMC Public Health 20, 1–6.

Zhang, M., Huang, G., Liu, C., Zhang, Y., Chen, Z., Wang, J., 2020. Distributions and origins of nitrate, nitrite, and ammonium in various aquifers in an urbanized coastal area, south China. J. Hydrol. 582. https://doi.org/10.1016/j.jhydrol.2019.124528.